Improving the Convergence Speed of the Resonator-Based Observer by Significant Component Selection

András Palkó, László Sujbert
Budapest University of Technology and Economics
Department of Measurement and Information Systems
Műegyetem rkp. 3., H-1111 Budapest, Hungary
Email: {palko, sujbert}@mit.bme.hu

***Abstract*—The resonator-based observer has been developed for measuring the harmonic components of a periodic signal with known fundamental frequency. In certain applications, the signal to be processed is sparse in the frequency domain: a subset of its harmonic components have negligible amplitude. This paper presents some extensions of the resonator-based observer which can exploit this sparsity to speed up the convergence. The performance of the proposed structures is demonstrated by simulation examples.**

***Index Terms*—periodic signals, order tracking, sparsity, convergence speed**

I. Introduction

In many applications, periodic signals are analyzed. Measuring their harmonic components is also known as order tracking [1]. Examples are active noise control, vibration analysis of rotating machines or line voltage harmonic analysis.

This problem can be approached in a model-based way. When the fundamental frequency is known and constant, the resonator-based observer (RBO) [2] is an adequate solution. The basic RBO has been already extended in multiple different ways. For unknown or changing fundamental frequency, the Adaptive Fourier Analyzer has been developed [3]. Another extension is the ability to handle missing samples [4].

Generally, a signal is said to be sparse if there is a basis in which it can be described with only a few nonzero coefficients. The notion of sparsity can be applied to periodic signals as well: strictly, it would mean that the majority of the Fourier coefficients are zero. In this paper, we will be more concessive: by sparse we mean that a non-negligible subset of the coefficients have (approximately) zero amplitude.

Trivial examples for sparse periodic signals are a pure sine wave, or a square wave with 50% duty cycle. A more practical example is the vibration caused by a ventilator: e.g. if it has five blades, then the 5th, 10th, 15th, ... components are expected to have significantly more power.

In this paper we present some extensions of the RBO which are able to exploit the sparsity of their periodic input signal in order to speed up the convergence. The core idea is to select those components which are presumably negligible, and exclude them from the main structure. The main characteristics of the structures are illustrated by simulations.

Project no. 2019-1.3.1-KK-2019-00004 has been implemented with the support provided from the National Research, Development and Innovation Fund of Hungary, financed under the 2019-1.3.1-KK funding scheme.

The structure of the paper is as follows: Section II reviews the RBO, while the proposed structures are presented in Section III. Section IV shows some examples, and the paper concludes in Section V.

II. Preliminaries

A. Conceptual Signal Model

The so-called conceptual signal model is the complex Fourier series of a periodic signal:

$$d = \sum_{k=-L}^{L} x_k \qquad x_k = X_k c_k \qquad c_k = \mathrm{e}^{\mathrm{j}2\pi f_1 k n} \tag{1}$$

for $k = -L, \ldots, L$, where X_k is the kth Fourier coefficient, x_k is the corresponding Fourier term, $\mathrm{j} = \sqrt{-1}$, f_1 is the fundamental frequency (relative to the sampling frequency), and n is the time index. In order to keep the notation clear, explicit time indices will not appear unless necessary.

Note carefully the difference between X_k and x_k. X_k is a Fourier coefficient, which is constant for a given periodic signal, while x_k is obtained by rotating X_k according to the frequency of the component and the time index.

The components are modeled up to the Nyquist frequency, thus $Lf_1 < 0.5 < (L+1)f_1$. The lack of modeled component at the Nyquist frequency poses no problem in practice.

Figure 1 depicts the conceptual signal model. The blue box is a block definition for further use. Each integrator also has a u_k update signal:

$$X_k(n+1) = X_k(n) + u_k(n) \tag{2}$$

B. Resonator-Based Observer

The RBO is obtained by designing a state observer for the conceptual signal model. As the state variables are the Fourier coefficients, the observer estimates them directly. The observer can be described by the following equations:

$$y = \sum_{k=-L}^{L} \hat{x}_k \quad \hat{x}_k = \hat{X}_k c_k \quad e = d - y \quad u_k = \tfrac{\alpha}{N} g_k e \tag{3}$$

$$g_k = \bar{c}_k = \mathrm{e}^{-\mathrm{j}2\pi f_1 k n} \quad (k = -L, \ldots, L) \tag{4}$$

DOI 10.3311/minisy2023-004

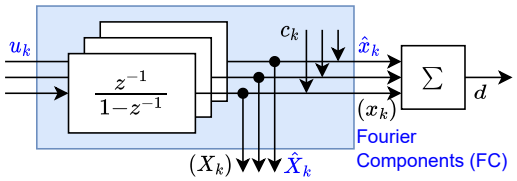

Fig. 1: The conceptual signal model. The blue box and its signals define the Fourier Components (FC) block and its interface for further figures. The equations in Section II-A use the X_k and x_k notation, all other equations and figures use the $\hat{X}_k$ and $\hat{x}_k$ notation.

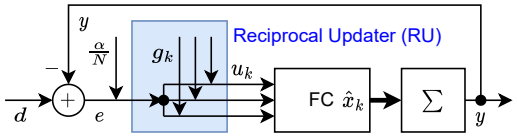

Fig. 2: The resonator-based observer. The blue box defines the Reciprocal Updater (RU) block for further figures. The thick line represents a vectorial signal. This convention is kept in further figures.

where y, e and d are the estimated input, error and input signals, respectively. $\hat{X}_k$ and $\hat{x}_k$ are the estimates of the kth Fourier coefficient and term, respectively, $0<\alpha\leq 1$, $N=2L+1$ is the number of modeled coefficients, g_k is a reciprocal complex exponential and $\bar{\cdot}$ denotes the complex conjugate.

The RBO is illustrated in Fig. 2. Here we define the Reciprocal Updater (RU) block. The modulation-demodulation scheme realized with c_k and g_k can falsely imply that the RBO is time variant. An equivalent formalization places the modulator-demodulator pair "inside" the integrator [5], which is clearly a time invariant system. These two equivalent formalizations also exist for the proposed structures.

In steady-state, the estimated and the original Fourier-coefficients are equal, thus the signal is perfectly reconstructed. The observer provides unbiased estimates of the Fourier coefficients [2].

If $0<\alpha<1$, the Fourier coefficient estimates are exponentially averaged [6] with an equivalent time constant of

$$\beta = 1-(1-\alpha)^{\frac{1}{N}} \tag{5}$$

We can see in (5) that for smaller N, the settling is faster, since there are less parameters to adapt.

For β small enough (which is usually granted in practical cases) the RBO is able to work over an arbitrary frequency set with similar convergence characteristics [6]. The "rows" in Fig. 2 (from u_k to $\hat{x}_k$ for a given k) are also called channels. Each channel corresponds to a single harmonic component. The magnitude response of any channel (from d to $\hat{x}_k$) is [6]

$$|H_k(f)| \begin{cases} =1 & \text{at the own frequency of the channel} \\ =0 & \text{at the frequencies of other channels} \\ >0 & \text{at any other frequency} \end{cases} \tag{6}$$

These relationships are illustrated for two cases in Fig. 3 (for $\hat{x}_2$). The blue line corresponds to a full RBO with $f_1=\frac{1}{15}$, $\alpha=1$. The 3rd and 6th components have been removed from this structure for the red line.

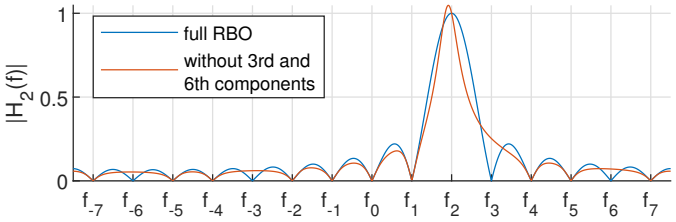

Fig. 3: Magnitude response of a single channel (from d to $\hat{x}_2$, on the interval $[-f_s/2, f_s/2]$). Blue line: full RBO with 15 channels. Red line: RBO with arbitrary frequencies.

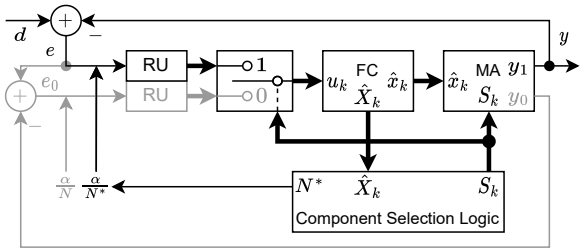

Fig. 4: RBO with significant component selection. The main loop is drawn with black, while the auxiliary loop is depicted in gray color.

III. The Proposed Structures

A. Concept

Let us consider a strictly sparse periodic signal and process it using the original RBO. In steady-state, there will be channels whose state variable will be zero. Removing them would have no effect on the estimated signal.

During the settling (with $0<\alpha<1$), each coefficient estimate (approximately) exponentially tends to their steady-state value. Assuming arbitrary initial state, after some time the magnitudes of the nonzero (zero) coefficient estimates will be significant (negligible).

The idea is to automatically distinguish between the significant and the negligible coefficients and their corresponding channels. Since the input can be described with only the significant coefficients, keep only them and drop the negligible ones from the main adaptation loop. Consequently, the main loop will contain less channels, which results in a faster convergence.

Moreover, it is conceivable that over time, the coefficients of the input signal change, some zeros become nonzeros or vice versa. Thus, the negligible components should not be dropped totally from the structure, but placed in an auxiliary loop and adapted there. If any of them becomes large enough, they can be placed back into the main loop.

B. Formalization

The basic proposed structure (Fig. 4, it will be referred as CSL+RU) can be described by formalizing the above ideas. There are two new blocks: the Component Selection Logic (CSL) and the Multiplexed Adder (MA).

Let us define the selection indicator for $k=-L,\ldots,L$:

$$S_k = \begin{cases} 1 & \text{if the } k\text{th component is significant} \\ 0 & \text{if the } k\text{th component is negligible} \end{cases} \tag{7}$$

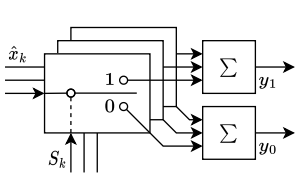

(a) Multiplexed Adder (MA)

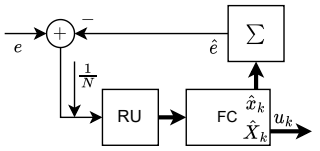

(b) Error Decomposition Updater (EDU)

Fig. 5: Block definitions for the proposed structures

The Component Selection Logic provides this indicator along with the $N^* = \sum_{k=-L}^{k=L} S_k$ number of selected components.

An MA (Fig. 5a) is used to calculate the y and y_0 output signals of the main and auxiliary loops, respectively:

$$y = \sum_{k=-L}^{L} \hat{x}_k S_k \qquad y_0 = \sum_{k=-L}^{L} \hat{x}_k \left(1 - S_k\right) \tag{8}$$

The two error signals are

$$e = d - y \qquad e_0 = e - y_0 \tag{9}$$

The update signals of the two loops can be expressed in one equation:

$$u_k = \tfrac{\alpha}{N^*} S_k g_k e + \tfrac{\alpha}{N} \left(1 - S_k\right) g_k e_0 \tag{10}$$

Note that the definition of S_k implies that the state variables are updated separately.

C. Discussion

The main loop is an RBO with an arbitrary (but special) frequency set. Since $N^* \leq N$, the convergence is faster than that of the original RBO. If the user knew which components are significant, he could use a traditional RBO with frequencies set to those components. The main novelty of this approach is that it detects the orders of significant components without user interaction. Moreover, the increase in convergence speed is independent from the orders of the significant components. They can be arbitrarily grouped or scattered over the spectrum.

For noise suppression in the main loop, the results of [6] apply, with N^* instead of N in the formulas. The variance of a given significant coefficient is inversely proportional to N^* (this variance is not less than in the original RBO). As a consequence, the summed variance of the coefficients in the main loop (which is related to the variance of y by Parseval's theorem) is approximately independent of the sparsity. In other words, the noise bandwidth from d to y is the same as that of in the original RBO.

In Fig. 4 the auxiliary loop is drawn as running on the error signal. An equivalent point of view is that the output of the auxiliary loop contains all channels and its input is d, not e. This is the reason this loop uses N in the update equation.

D. Component Selection Logic

The responsibility of the CSL is to provide the selection indicator, i.e. distinguish between the significant and the negligible components. In this paper, we take a simple thresholding approach. This threshold can be a fixed value, given a priori, or it can be dynamic, e.g. based on the coefficient with maximal magnitude:

$$S_k = \begin{cases} 1 & \text{if } |\hat{X}_k| \geq \gamma |\hat{X}|_{\max} \\ 0 & \text{else} \end{cases} \tag{11}$$

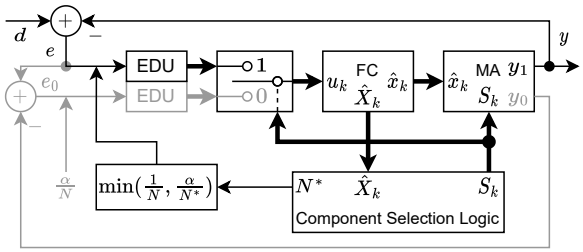

Fig. 6: The proposed structure with error signal decomposition

where $0 < \gamma \ll 1$. Hysteresis can be used in order to eliminate the "juggling" of components between the two loops.

E. Error Signal Decomposition

Let us consider the case when besides the significant components, there are small (but not zero) ones in d, and they do not get selected. Alternatively, let us consider the effect of selection errors.

Let one not selected nonzero component be the ith one and let us examine its effect on the kth (selected) component. The magnitude response of the main loop has the characteristics outlined in (6). Consequently, $|H_k(f_i)| > 0$. This means that the not selected component at f_i causes an error in the measurement of the selected component at f_k.

For a particular example, let us take the case depicted with the red line in Fig. 3 and consider the effect of the not selected nonzero 3rd component on the selected 2nd one. Since $|H_2(f_3)| \approx 0.25 > 0$, this component at f_3 causes an error in the measurement of the selected component at f_2.

Thus the not selected nonzero components cause some error in the measurement of the selected components. As a result, the selected components do not vanish entirely from e. With a similar reasoning one can see that in this case the precision of the auxiliary loop is also impaired.

This problem can be solved via the decomposition of the error signal. The structure is modified slightly: instead of the RU blocks, an Error Decomposition Updater (EDU, Fig. 5b) is used in both loops (Fig. 6). The EDU is a full RBO run on e with $\alpha = 1$, and the Fourier coefficient estimates are taken as update signals. This variant will be referred as CSL+EDU.

Since the EDU is a full RBO, its magnitude response from e to u_k is characteristically same as the blue line in Fig. 3, regardless of the actual selection. Now $|H_k(f_i)| = 0 \, (i \neq k, i = -L, \ldots, L)$, thus the not selected nonzero components do not cause error in the measurement of the selected ones. For our particular example, the blue line in Fig. 3 has a zero at f_3, thus no component appears in u_2.

Since there is a new feedback loop inside the main loop, the $\frac{\alpha}{N^*}$ gain of the main loop cannot get as large as for CSL+RU. In our experience, an upper bound of $\frac{\alpha}{N^*} \leq \frac{1}{N}$ yields similar convergence to the CSL+RU.

IV. Examples

The examples model the measurement of the significant harmonic components of the line voltage. As such, the input signal will have 50 Hz frequency, sampled at 5 kHz. The fundamental component has a magnitude of 1 and there is no bias. The examples will differ in the higher harmonics.

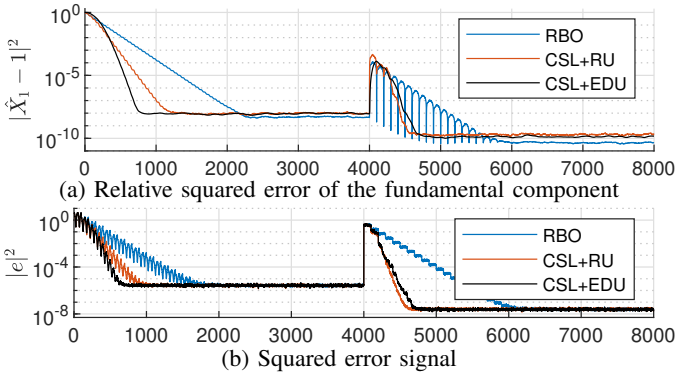

(a) Relative squared error of the fundamental component

(b) Squared error signal

Fig. 7: Measurement errors by the time index for strictly sparse signals, averaged from 100 simulations

A. Strictly Sparse Signal

In the first example, the input signal is strictly sparse. In the beginning, the even harmonics are zeros, while the odd ones have a random magnitude drawn uniformly from $[0.05, 0.1]$ and a random phase. After 4000 samples, the harmonic components change: the odd ones become zeros and the even ones up to the 20th order get a random magnitude and phase the same way as the even ones before. There is an additive white Gaussian noise on the input, with 60 and 80 dB SNR in the two signal parts.

This signal is processed using the original RBO, CSL+RU and CSL+EDU. All structures use $\alpha = 0.35$. The CSLs are operated by (11) with $\gamma = 0.02$, 4 times per signal period.

100 such simulations were conducted. The averaged relative squared error of the fundamental component is shown in Fig. 7a. Both proposed structures are able to speed up the convergence. Although there is an upper bound on the feedback gain of CSL+EDU, it was even faster than the CSL+RU. This acceleration depends also on the sparsity of the signal: the less components a signal has, the faster the convergence is for the proposed structures (the error of the proposed structures decays faster for the sparser signal part; the RBO is unaffected by the sparsity). The proposed structures have only slightly worse steady-state error than the RBO, due to their larger noise bandwidth.

The error signals (Fig. 7b) show the same convergence characteristics as the selected component estimates. Moreover, the steady-state reconstruction error is the same for all structures.

At the signal change point, the fundamental component is unchanged. As a result, its error jumps only because the other components affect it during the transient. After such an abrupt change in the Fourier coefficients, some time is needed for the CSL to actualize the selection (since the corresponding component estimates need to change). During the settling, some channels may be placed back and forth multiple times.

B. Effect of Small Components

The second example illustrates the effect of the small components. The input signal has the same parameters as in the first half of the previous example, with one exception: the small components are not zero, but have a magnitude drawn independently from a normal distribution with zero mean and

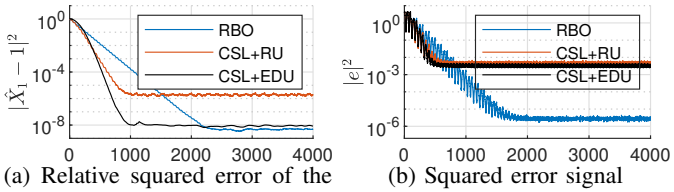

(a) Relative squared error of the fundamental component

(b) Squared error signal

Fig. 8: Measurement errors by the time index for for signals with significant and small components, averaged from 100 simulations.

0.01 standard deviation, and a random phase. The structures and their parameters are the same as before.

Again, results from 100 simulations were averaged to obtain the results. For the fundamental component estimate (Fig. 8a), CSL+RU has a significantly higher error than the other structures, the original RBO included: the not selected nonzero components cause an error in the selected ones. CSL+EDU has only slightly worse error than the RBO, due to its larger noise bandwidth. Moreover, as in the previous example, the proposed structures have faster convergence.

It is not surprising that CSL+RU has a higher steady-state reconstruction error than the RBO (Fig. 8b). But one could expect the CSL+EDU to have significantly lower error than the CSL+RU. This is unfounded though: even when all selected components are measured perfectly, the error signal of the main loop contains all the small components by design.

V. Conclusion

This paper presented two structures to improve the convergence speed of the RBO for sparse periodic signals. After reviewing the original RBO, the proposed structures have been presented. The core idea is to automatically separate the significant and negligible components, and measure only the significant ones in the main loop Little additional complexity is required: parallel and/or series connected resonators, adders, switches and some control logic. Since this way there are fewer parameters to adapt, the convergence becomes faster. The properties of the proposed structures were demonstrated with simulation examples: they converge faster than the original, and the speed depends on the sparsity of the input. Using error signal decomposition, the left out nonzero components cause no error in the measurement of the selected ones.

References

[1] A. Brandt, T. Lagö, K. Ahlin, and J. Tůma, "Main principles and limitations of current order tracking methods," *Sound & vibration*, vol. 39, pp. 19–22, 03 2005.

[2] G. Peceli, "A common structure for recursive discrete transforms," *IEEE Trans. Circuits Syst.*, vol. 33, no. 10, pp. 1035–1036, 1986.

[3] L. Sujbert, G. Simon, and G. Peceli, "An observer-based adaptive fourier analysis [tips & tricks]," *IEEE Signal Process. Mag.*, vol. 37, no. 4, pp. 134–143, 2020.

[4] G. Orosz, L. Sujbert, and G. Peceli, "Analysis of resonator-based harmonic estimation in the case of data loss," *IEEE Trans. Instrum. Meas.*, vol. 62, no. 2, pp. 510–518, 2013.

[5] Z. Kollar, F. Plesznik, and S. Trumpf, "Observer-based recursive sliding discrete fourier transform [tips & tricks]," *IEEE Signal Process. Mag.*, vol. 35, no. 6, pp. 100–106, 2018.

[6] L. Sujbert, G. Peceli, and G. Simon, "Resonator-based nonparametric identification of linear systems," *IEEE Trans. Instrum. Meas.*, vol. 54, no. 1, pp. 386–390, 2005.